Egypt. J. Soil Sci. **Vol. 61,** No. 4, pp. 433 - 444 (2021)

Egyptian Journal of Soil Science

http://ejss.journals.ekb.eg/

Effect of Calcination and Ca-modified on Bentonite and Zeolite, with Respect to Phosphorus Removal from Aqueous Solution

Ahmed A. El-Refaey

Department of Soil & Water Science, Faculty of Desert and Environmental Agriculture, Matrouh University, Egypt

Abstract

The effect of the thermal treatment and Ca-modification on bentonite (Bent) and zeolite (Z) was investigated for the ability of phosphorus sorption. Bentonite and zeolite were characterized by X-ray diffraction (XRD), X-ray fluorescence (XRF), Brunauer Emmett Teller (BET) specific surface area, Fourier transform infrared (FTIR), scanning electron microscopy (SEM), and energy dispersive spectroscopy (EDX). The XRD analysis indicated that montmorillonite and clinoptolite were the main minerals in bentonite and zeolite, respectively. Bentonite and zeolite were exposed to calcination and hydrothermal treatments with $CaCl_2$ (0.1M) at different temperatures (200, 400, 600, 800, and 1000^{o}C) for 2 hr. The final reaction products were inspected, by XRD, FTIR, SEM, and EDX.The result of the thermal treatments was a significant loss of crystallinity and their structure in calcination than in hydrothermal treatments as a possible consequence of the increase of calcium ions and changing the Si/Al ratio. Further, batch equilibrium experiments were carried out at room temperature (25^{o}C) for 24 hr to investigate the effect of thermal treatment of Bent and Z for their ability for phosphorus sorption. The removal ability of phosphorus decreased with the increasing temperature of the thermal treatment of the sorbents as a result of the decreases in pore volume, and surface area. Bent and Z hydrothermal treatments less than 1000^{o}C indicated the enhancement effect of the calcium bending minerals on phosphorus removal ability.

Keywords: Calcination; Hydrothermal; Bentonite; Zeolite; Phosphorus

Introduction

Bentonite and zeolite are well-known, efficient, and environmentally-friendly sorbents (Westholm 2006; Ahmaruzzaman, 2008; Moharam and Jalali, 2013 and 2015). Bentonite is a dominant term used for smectite minerals. Smectites are 2:1 layer minerals, where have two silica tetrahedral sheets joined to central octahedral sheets. Montmorillonite is the dominating mineral composing smectite (Murray, 2007). Bentonite has been used as a soil amendment especially, in sandy soils (Hilal and Helal, 2013; El-etr et al., 2016). Because of its physicochemical characteristics, bentonite can be used in the remediation process (Bloom, 2000; Stagnaro et al., 2012). Therefore, the consumption of clays as adsorbents for removing pollutants has been increasing attention due to readily available, low-price, and Eco-friendly. Additional benefits for using clay as adsorbent materials are associated with intrinsic characteristics such as surface area, good physical and chemical stability, and a variety of structural characteristics (Kubilay et al., 2007; Chen et al., 2008). Also, clay minerals can be used as a chemical barrier that can attenuate hazardous pollutants migration and a physical barrier because of the adequacy of clay to swell, seal cracks (Sellin and Leupin, 2014).

Zeolite is an aluminosilicate mineral composed of the tetrahedral framework, coordinated with mutual oxygen atoms. Zeolite has a porous and regular structure. Due to excellent sorption properties, large surface area, and high cation exchange capacity,

*Corresponding author e-mail: ahmedelrefaey@alexu.edu.eg
Rceived: 6/12/2021; Accepted: 1/2/2022
DOI: 10.21608/ejss.2022.108515.1482

zeolites are commonly used for the purification of wastewaters, air purification, soil amendment, animal nutrition, aquaculture, heat storage and solar refrigeration, and catalysts (Wingenfelder et al., 2005; Leggo et al., 2006; Salem et al., 2012; Gomah, 2015;Nakhli et al., 2017).

Mineral calcination has got wide attention due to its influence on mineral characteristics and its applications (Harvey and Lagaly, 2013; Claverie et al., 2015). Calcination is defined as the heating process to high temperatures in presence of air or oxygen (IUPAC, 1997). Temperature and time of calcination are accountable for activation of the aluminosilicate contents (Murat and Comel, 1983; Darweesh et al., 2007, Mara et al., 2016). Hydrothermal process denotes heterogeneous reactions in aqueous media above 100°C and 1bar. Hydrothermal processes take place in minerals formation by nature and industry of materials synthesis (O'Hare, 2001). The hydrothermal method has numerous privileges such as simplicity, better nucleation control, higher rate of reaction, highly crystalline, and better shape control (Yoshimura and Byrappa, 2008; Byrappa and Yoshimura, 2013). Effect of thermal treated and hydro-calcination on bentonite and zeolite has the attention with affecting their adsorption capacity. Substrates with high content of calcium have the potential to be phosphorus-removing absorbents (Kõiv et al, 2010; Vohla et al., 2011; Jowett et al., 2018).

Reducing phosphorus concentrations in the environment and receiving water body is considered to be the most effective way to control nutrient contamination and water eutrophication. Eutrophication became a worldwide environmental thread and attracted the attention of scientists and governments. Persistent algal blooms in aqua and coastal areas could make many ecological, economic, and social threads. In Aqua ecosystems, phosphorus comes basically from point and non-point sources, such as industrial effluents, sewerage, and agricultural runoff, in addition to sediment flux (Xiong and Peng, 2008; Wei et al., 2008; Rentz et al., 2009; Yin et al., 2011).

Therefore, the purpose of this study was to compare and track the changes induced by calcination and Ca-modified by hydrothermal treatment with $CaCl_2$ (0.1M)at various temperatures (200, 400, 600, 800, and 1000^{o}C)on bentonite and zeolite properties, and their ability for phosphorus sorption.

Materials and methods

Materials

Natural bentonite and zeolite were obtained from Egypt Company for Mining and Drilling Chemicals. Minerals samples were grounded and passed through a 0.5 mm sieve and kept in plastic jars for future analysis.

Thermal and hydrothermal reactions were performed in the muffle in ceramic vessels. The thermal treatment was conducted by subjecting the minerals (bentonite and zeolite) to calcination in muffle at 200, 400, 600, 800, and 1000^{o}C for a period of 2 h. Also, bentonite and zeolite were hydrothermally treated in a $CaCl_2$ (0.1M) solution as a calcium source (1:50 w/v) and then heated for the same temperatures (200, 400, 600, 800, and 1000^{o}C) for 2 h.

Part of the calcination samples, 2.00g sample, was treated with 100 ml $CaCl_2$ (0.1M)and shacked for 2h, and then washed and filtered for phosphorus sorption test.

Materials characterization

The crystal chemistry characteristics for bentonite and zeolite were conducted by X-ray powder diffraction (XRD), and X-ray fluorescence (XRF) spectroscopy on bentonite and zeolite samples. XRD was determined for bentonite and zeolite at original, calcined, and after hydrothermal states using X-ray Powder Diffraction-XRD-D2 Phaser Bruker (Germany) using the Cu Kα radiation ((λ=1.541 Å) at 30 kV and 10 mA. The diffractogram was scanned from (2θ) 5 to 45◦.

Bentonite and zeolite element composition was recognized by X-ray fluorescence spectroscopy (XRF) using Axios advanced sequential wavelength dispersive X-ray fluorescence Spectrometer (Malvern Panalytica) (Table 1).

Emmett–Teller specific surface area (SSA_{BET}) for bentonite and zeolite were determined using N_2-adsorption isotherms (Beckman Coulter SA (TM) 3100). Also, The Barrett–Joyner–Halenda (BJH) method from the N_2 desorption isotherms was conducted for identifying the pore size distribution (Nader, 2015).

The Fourier transform-infrared (FTIR) spectra were conducted for the raw bentonite and zeolite, as well as after calcination and hydrothermal treatment with $CaCl_2$ (0.1M) at the range 400 – 4,000 cm^{-1} by a Fourier transforms infrared spectrometer (Infra-Red Bruker Tensor 37, German) applying KBr pellet method.

Surface morphologies examination of bentonite and zeolite were performed by a Jeol IT-200 scanning electron microscope. Samples were covered with gold in a sputter-coating unit (JFC-1100E) before the examination. Scanning electron microscopy (SEM) images were gained at various magnification scales with different thermal treatments.

For energy dispersive X-ray (EDX) analysis, samples without gold coating were examined and the element surface percentage content was taken as an average of three examined fields.

Batch studies

A primary experiment was conducted to evaluate the phosphorus sorption ability of bentonite and zeolite before and after different thermal and hydrothermal treatments. A 0.50 g of the sorbent was added into 25 ml of the phosphorus solution (200 mg/l) at pH 7.00 and was shaken at 200 rpm for 24 h at room temperature (25 °C). The pH was adjusted by NaOH (0.1M) and HCl (0.1M). After equilibrium (24 h), the suspensions were centrifuged, filtered (Whatman No. 42), and measured for P concentration. Concentration of phosphorus was measured colorimetric by molybdenumblue method at wavelength 882 nm using JENWAY 6105, UV/VIS spectrophotometer (Olsen and Sommers, 1982).

Results and Discussion

Chemical composition and minerals phases

The main compositions of bentonite and zeolite as identified by X-ray fluorescence spectroscopy (XRF) are presented in Table 1. Normally, SiO_2 and Al_2O_3 are the main compositions in bentonite and zeolite with other oxides (Table 1). The content ofAl_2O_3, Fe_2O_3, and Na_2O in bentonite was higher than the content in zeolite. Otherwise, zeolite contents of SiO_2, CaO, and K_2O were higher than in bentonite. Zeolite has extensively various Si: Al ratios that could help in the recognition of separate species. Si: Al ratio, in zeolite sample, equals 6.17 (≥ 4.0) which referred to clinoptilolite as indicated by XRD reflection (Snellings et al., 2003). The XRD reflections for bentonite and zeolite are shown in Fig. 1 and 2. The XRD pattern showed that montmorillonite is the key dominant mineral phase for natural bentonite (El Refaey, 2021). Also, the presence of quartz, and calcite as impurities were identified (Fig.1). Obviously, clinoptolite; was the main mineral in zeolite composition (Seraj et al., 2016) with quartz and cristobalite as impurities (Fig. 2).

Surface area and pore analysis

Figure 3 illustrated the increase of the adsorbed amount of N_2 with the rising of relative pressures (P/Po) between 0.1 and 0.9 for bentonite and zeolite. The obtained Brunauer Emmett Teller specific surface area (SSA_{BET}) of bentonite (44.78 m^2g^{-1}) was greater than zeolite (28.57 m^2g^{-1}). The desorption BJH pore size distribution for bentonite and zeolite is listed in Table 2. According to the International Union of Pure and Applied Chemistry (IUPAC), micropores are pores with less than 2 nm width; mesopores are 2 to 50 nm width, and more than 50nm for macropores (Rouquerol et al., 1994; Yahya et al., 2015). From the available results, the pore diameter of < 6 nm, which is related to micropores was higher (81.71%) than bentonite (50.41%)(Table2). Zeolite has been reported as mainly meso-porosity formed from the space between crystal aggregates (Elaiopoulos et al., 2010; Seraj et al., 2016). The framework of bentonite and zeolite have a net negative charge because of the substitution of Al^{3+} for Si^{4+} in the aluminosilicate tetrahedra, which is balanced by exchangeable cations in the mineral pores (Elaiopoulos et al., 2010; Seraj et al., 2016).

TABLE 1. Main constituents of bentonite (Bent) and zeolite (Z)

	Main Constituents (wt%)							
	SiO_2	TiO_2	Al_2O_3	Fe_2O_3	MgO	CaO	Na_2O	K_2O
Bent	49.17	0.22	14.55	7.37	2.23	0.75	3.25	0.68
Z	71.00	0.25	11.50	1.80	0.55	1.75	0.75	3.50

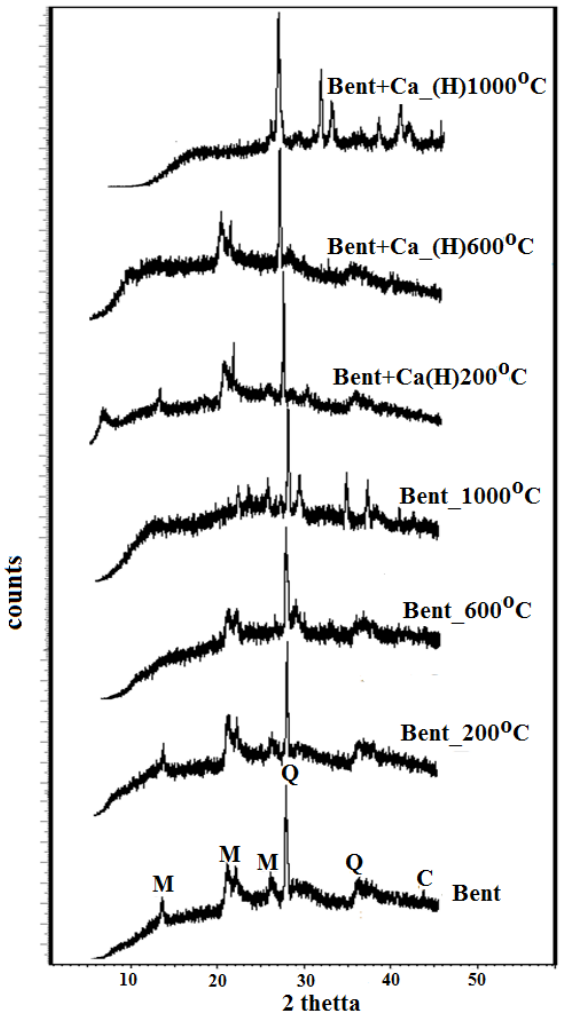

Fig. 1.XRD patterns of bentonite (Bent), calcined, and hydrothermal (H) treatments with $CaCl_2$(0.1M) ones at 200, 600, and 1000°C
(C: Calcite; M: Montmorillonite; Q: Quartz)

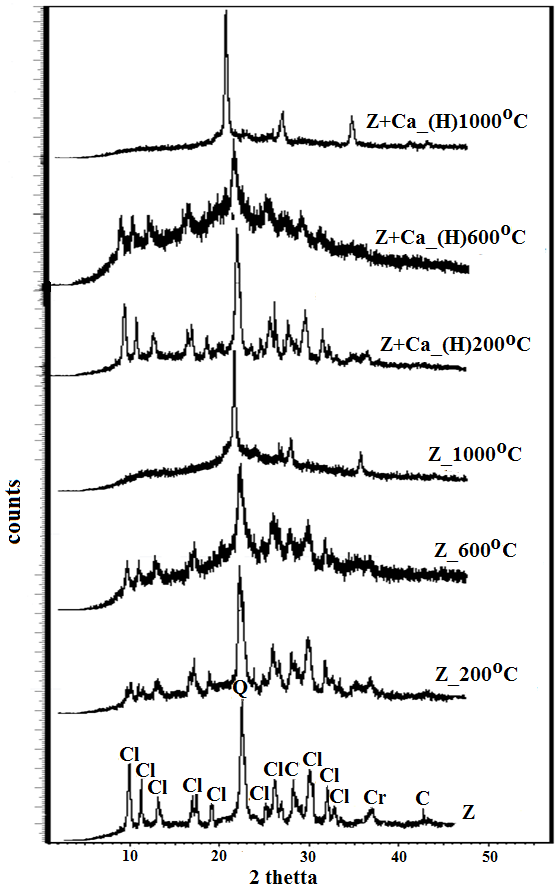

Fig. 2. XRD patterns of zeolite (Z), calcined, and hydrothermal (H) treatments with $CaCl_2$(0.1M) ones at 200, 600, and 1000°C (C: Calcite, Cl: clinoptolite; Cr: cristobalite; Q: Quartz)

XRD tracking results

XRD analysis is a valuable tool for qualitative tracking of modifications in crystal structure produced by calcination and hydrothermal (Elaiopoulos et al, 2010). Dehydroxylation during calcination could convert clay minerals into a metastable state and the structure became a non-crystalline metastable state (D'Eliaa et al. 2018, Erdemoğlu et al., 2020). As outlined by Grim and Guven (1978), the reactions could occur to smectite during calcination. Initially, all clays lose the pore water at 100 to 150°C, and with raising the temperature to 300°C and smectites lose the expanding characteristic. By raising the temperature between 450 to 700°C, the hydroxyl water from the lattice is lost. So, Bentonite with dominated montmorillonite mineral expected to the destruction of lattice structure and no shrinkage with the loss of hydroxyl water with increasing temperature above 900°C (Grim, 1968; Grim and Guven, 1978).

Change of the intensity of the dominant peaks in the XRD patterns could be used to estimate the modified and crystallinity loss of the minerals (Elaiopoulos et al, 2010). As increasing the calcination temperatures, the XRD pattern of bentonite showed a decrease in the intensity peaks of montmorillonite (Fig. 1). That could be due to dehydroxylation and collapse of the clay structure that turned into amorphous material.

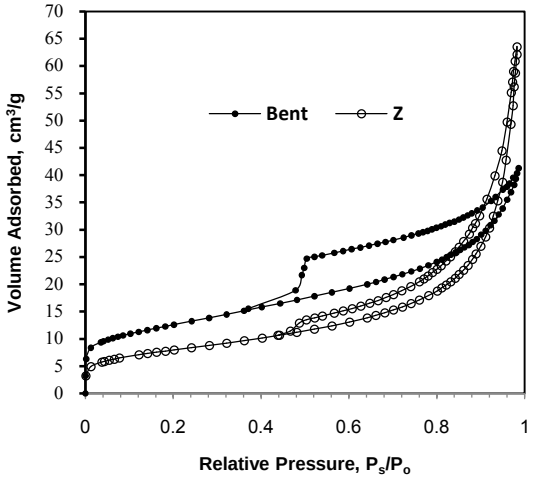

Fig. 3. N_2-adsorption isotherms of bentonite (Bent) and zeolite (Z).

TABLE.2 Desorption Barrett-Joyner-Halenda (BJH) pore size distribution for bentonite (Bent) and zeolite (Z)

Pore diameter range nm	Pore volume			
	Bent		Z	
	ml g^{-1}	%	ml g^{-1}	%
< 6	0.02632	49.59	0.01255	12.28
6 - 8	0.00330	6.22	0.00487	4.76
8 - 10	0.00192	3.62	0.00364	3.56
10 - 12	0.00234	4.41	0.00501	4.90
12 - 16	0.00248	4.67	0.00690	6.75
16 - 20	0.00273	5.15	0.00849	8.30
20 - 80	0.01103	20.78	0.04780	46.75
> 80	0.00295	5.56	0.01298	12.69

Also, the XRD pattern showed diminish of carbonate mineral because of its decomposition by increasing calcination temperatures, however, carbonate thermally disassociated into CaO and CO_2 at 600–800°C (Zhang et al., 2019). While quartz peak in the XRD patterns was stabled with increasing the calcination and hydrothermal temperatures (Fig. 1).

Calcination of zeolite would lower pores water content, as the destabilization of crystal latticework would decrease the porosity of the zeolite and thereby lower the amount of water being absorbed into the micropores and mesopores (Seraj et al., 2016). After calcination at 200, 600, and 1000°C, the XRD pattern for zeolites presented that the intensity peaks of clinoptilolite reduced significantly with increasing in calcination temperatures (Fig. 2). This reduction in crystallinity indicated the collapse of the mineral structure. Also, calcite peak intensity was decreased as a result of mineral decomposition. Clearly, quartz, cristobalite, and were able to be stable with

increasing the calcination and hydrothermal temperatures (Fig. 2).

On other hand, XRD results of hydrothermal treatments with $CaCl_2$ showed in Fig. 1 for bentonite and Fig. 2 for zeolite with different temperatures (200, 600, 1000^oC) compared with original minerals. Fairly, high temperatures (<1000^oC) did not make significant changes in the structure of bentonite or zeolite compared with the original mineral as shown in Fig. 1 and 2. The presence of Ca^{++} ions could support the stability of the crystal structure upon heating. The framework Si/Al ratio and the ion-exchangeable cations in hydrothermally dealumination suggested that playing a dominant factor, and could affect the structural stability and exhibit different dehydration behavior (Gonzalez-Velasco et al.,2000; Elaiopoulos et al., 2010).

The presence of $CaCO_3$ peaks in both bentonite and zeolite after hydrothermal treatment at 1000^oC could be a possibility small growth reform by in-situ reaction between the freshly-formed CaO with CO_2 in the environment and that could affect the porous structures (Zhang et al., 2019).

FTIR analysis

The FTIR spectra of bentonite, as well as zeolite, and after calcination and hydrothermal treatment by $CaCl_2$ (0.1M) including the bands corresponding to stretching and bending vibrations, are shown in Fig. 4 and 5. For bentonite FTIR spectra, the bands at 3622.10 cm^{-1} and 914.78 cm^{-1} confirm the presence of dioctahedral smectite mineral with Al–OH–Al (Toor et al., 2015; Kumararaja et al., 2017).The band at 3697.22 cm^{-1} was attributed to Al-Mg-OH stretching while vibration at 791.10 cm^{-1} confirmed the presence of quartzin the bentonite clays (Vieiraa et al., 2010). Also, vibration at 696.03 cm^{-1} was associated with Si-O-Al vibration (Ayari et al., 2007; Kumararaja et al. 2017; Al-Essa, 2018). The peaks at1034.16 cm^{-1}, 532.75cm^{-1}, and 468.33 cm^{-1} were assigned to the Si–O stretching vibration of bentonite mineral (Paluszkiewicz et al., 2008; Benhouria et al., 2015; Kumararaja et al., 2017). The broad bands at 3442.46 cm^{-1} and 1639.72 cm^{-1} are attributed to the stretching vibrations of O–H stretching in the bentonite (Toor et al., 2015; Shehata et al., 2016; Ravindra et al., 2017). The peak at1464.65 cm^{-1} corresponded to C-H stretching (Pavia et al., 2009; Anirudhan and Ramachandran, 2015).

The infrared spectra of zeolite showed that the peak at 1209.20 cm^{-1}, 1059.63cm^{-1}, 522.94cm^{-1}, and 465.47 cm^{-1} were the bending vibration peak of Si–O corresponds to the filosilicate structure (Li et al. 2008; Paluszkiewicz et al., 2008; Benhouria et al., 2015; Kumararaja et al., 2017). The stretching band of 730.23 cm^{-1} could be assigned to $(CO3)^{2-}$group (Udvardi et al., 2014; Mroczkowska-Szerszeń and Orzechowski, 2018). The transmission at 675.12cm^{-1} and 607.38 cm^{-1} were related to Si–O–Al group (Salem et al., 2012; Ayari et al., 2007; Kumararaja et al. 2017; Al-Essa, 2018). The stretching vibration Al-Fe-OH bending was located at 792.02 cm^{-1}. The broad band's at 3440.85 cm^{-1} and 1634.37 cm^{-1} attributed to the O–H stretching of interlayer water molecules in zeolite (Novaković et al., 2008; Toor et al., 2015; Shehata et al., 2016; Ravindra et al., 2017).

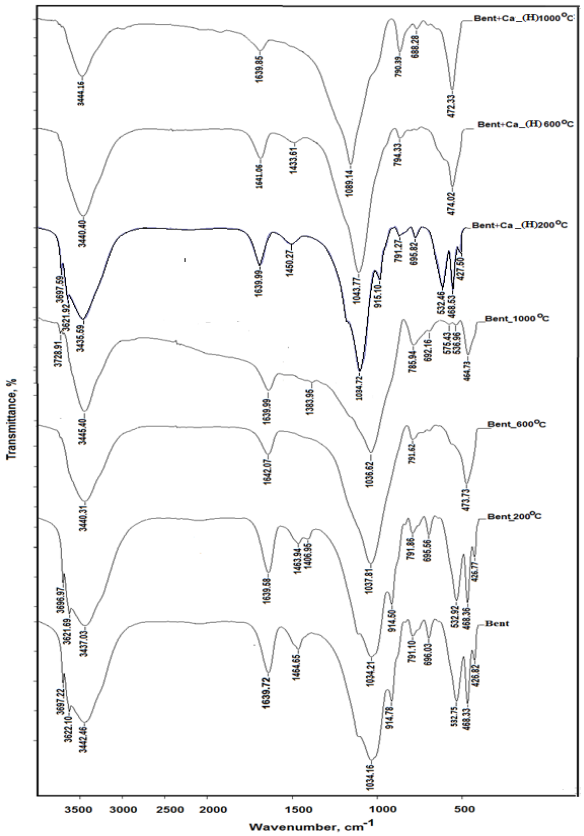

Fig. 4. Infrared spectra of natural bentonite (Bent),calcined, and hydrothermal (H) with $CaCl_2$ (0.1M) ones at 200, 600, and 1000^oC

FTIR analysis could assist in tracking the changes of structural after the thermal treatments (Vieiraa et al., 2010). From the FTIR spectra results, it could be shown that there was a deviation in bands positions after thermal and hydrothermal treatments in both minerals. FTIR result suggests the displacement of water by thermal treatment. However, OH^- stretching vibrations and bands related to the presence of water molecules in bentonite and zeolite displayed decreased intensity and disappeared for others related (such as 3697.22, 3622.10, and 914.78 cm^{-1} for bentonite and 3624.08, 732.23, and 675.12 cm^{-1} for zeolite) after the calcination and hydrothermal process. That could point out the incident of dehydration and dehydroxylation by thermal treatments as indicated by XRD analysis. Also, it could be shown from FTIR analyses that peaks related to carbonate at 1464.66, and 1389.09 cm^{-1} in

bentonite and 732.23 cm^{-1} in zeolite disappeared with increasing thermal process. As reported by Cinku et al. (2014) and Zhang et al. (2019) and indicated by XRD analyses that carbonate thermally disassociated at 600–800°C. The bands assigned by the presence of quartz in both bentonite and zeolite (791.10 and 792.02 cm^{-1}, respectively) did not nearly modify their position after thermal or hydrothermal treatments (Fig. 4 and 5).

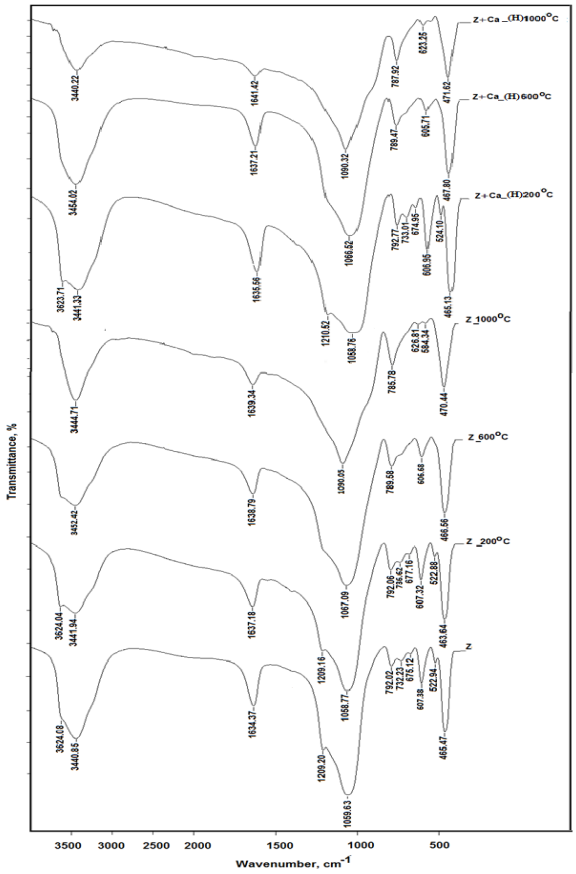

Fig. 5. Infrared spectra of zeolite (Z), calcined, and hydrothermal (H) treatments with $CaCl_2$ (0.1M) ones at 200, 600, and 1000°C

Scanning electron microscopy (SEM)

The SEM images showed the surface morphology of bentonite and zeolite and its changes after calcination and hydrothermal treatments with $CaCl_2$ (0.1M)at different temperatures (Fig.6). SEM image demonstrates that bentonite has a clear plate with lamellar curly surface morphology (El Refaey, 2021). SEM of zeolite revealed the porous structure and rough surface with the uniform size distribution of the crystals. This could be expected because the precursors are shielded from aggregation during crystallization. The structure of bentonite and zeolite was significantly modified during the thermal treatment and the difference in morphology of natural bentonite and zeolite before and after calcination and hydrothermal treatments was clearly observed. Structural collapse was obviously visible with increasing the temperature of calcination than with hydrothermal treatments with CaCl (0.1M). As it can be observed in Fig. 6, densest microstructure, more compacted, and reduced the interlamellar spacing is obvious with increasing the temperature and could be explained by changes in the pore structure as a result of removing of OH groups from the structure which could not be detected by x-ray diffraction analysis (Rossetto et al. 2009, Anadão et al. 2014; Nones et al. 2015; Santos et al., 2019; Erdemoğlu et al., 2020).

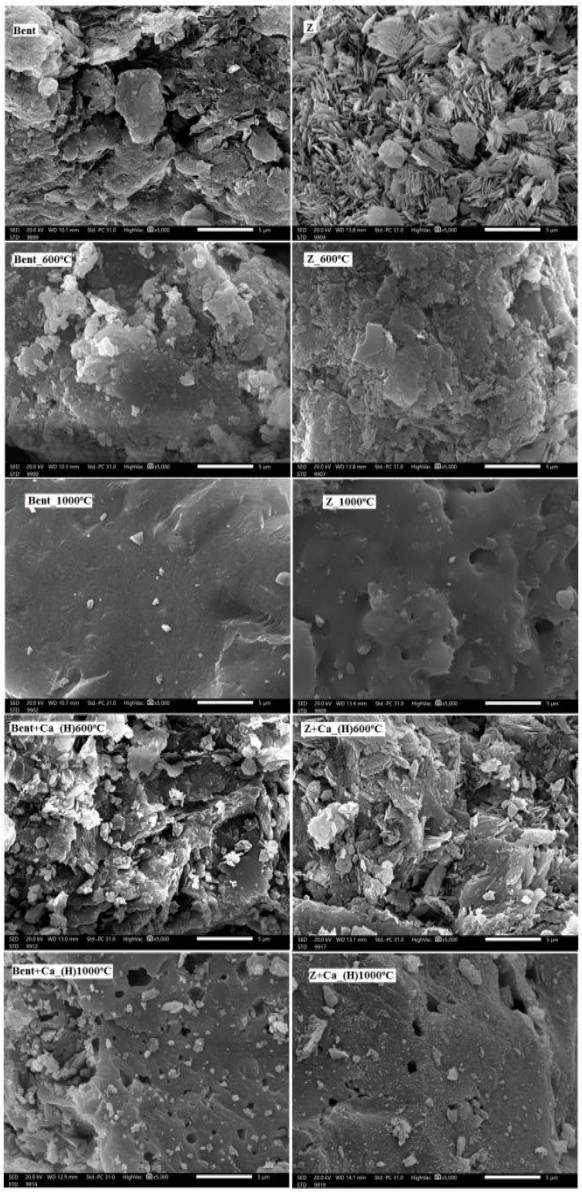

Fig.6. SEM photos of natural bentonite (Bent), zeolite (Z), the calcined and hydrothermal (H) treatments ones at 600, and 1000°C

EDX analysis

The molecular composition of compounds on bentonite and zeolite in natural, calcined, and hydrothermal treatments are shown in Fig. 7 for bentonite and Fig. 8 for zeolite. EDX analysis is recognized peaks of oxygen (50.85%), silicon (19.62%), aluminum (9.10%), carbon (7.13%), iron (5.61%), sodium (2.84%), calcium (1.24%), magnesium (1.18%), titanium (0.79%), and potassium (0.68%) as ingredient elements of bentonite (Table 3). On other hand, the percent of the main element at the surface of zeolite were oxygen (55.00%), silicon (27.90%), aluminum (5.88%), carbon (5.72%), calcium (2.79%), iron (1.19%), potassium (1.03%), and magnesium (0.48%) (Table 4). As expected Si and Al oxides were the main elements. Also, EDX revealed a significant reduction of carbon contents with increasing temperature in calcination and hydrothermal treatments with Ca_2Cl (0.1M) as a result of the dissolution of carbonate mineral with raising the temperature as indicated by XRD results in both bentonite and zeolite (Fig. 1 and 2). Chloride percentage on the surface of bentonite diminished as a result of increasing temperature in calcination and hydrothermal treatments (Table 3).With the increasing temperature of the hydrothermal treatment process, Na percentage diminished and indicated the increases of Ca^{++} ions on the surface of bentonite, on other hand, Ca^{++}percentage increased at 600 ^oC for zeolite only and could explain P removal (Table 4). Si/Al ratio is one of the major parameters that monitor the deformation of the crystalline structure, where dealumination (decreasing of Al) can result in crystallinity loss (Kim et al., 2002; Lopez-Fonseca et al., 2003; Elaiopoulos et al., 2010). The Si/Al ratio increased with increasing temperature in calcination from natural mineral, 600 to 1000^oC (for bentonite 2.16, 2.41 and 3.01; and 4.74, 5.12, and 5.10 for zeolite) as indicating loss of crystallization and converting to amorphous state. Otherwise, Si/Al ratio accomplished with hydrothermal treatment of bentonite slightly increased (2.60), suggesting that the presence of Ca^{++} ions could be a service of the stability of the crystal structure upon increasing temperature (Table 3).On other hand, Si/Al ratio accomplished with hydrothermal treatment for zeolite did not have aclear trend, but a lower Si/Al ratio was3.44 with hydrothermal treatment at 600^oCcompared with others(Table 4).

Effect of thermal and hydrothermal treatments on P-removal

The effect of thermal treatments on phosphorus sorption ability compared to hydrothermal treatment with $CaCl_2$ (0.1 M) for bentonite (Bent) and zeolite (Z) is shown in Fig. 9. As shown from the results, the sorption ability for phosphorus decreased with the increasing temperature of the thermal treatment of the minerals with the privilege for bentonite than zeolite, and hydro-calcination with $CaCl_2$ (0.1M) than calcinated sorbents and calcination sorbents treated with $CaCl_2$ (0.1M) (Fig. 9).

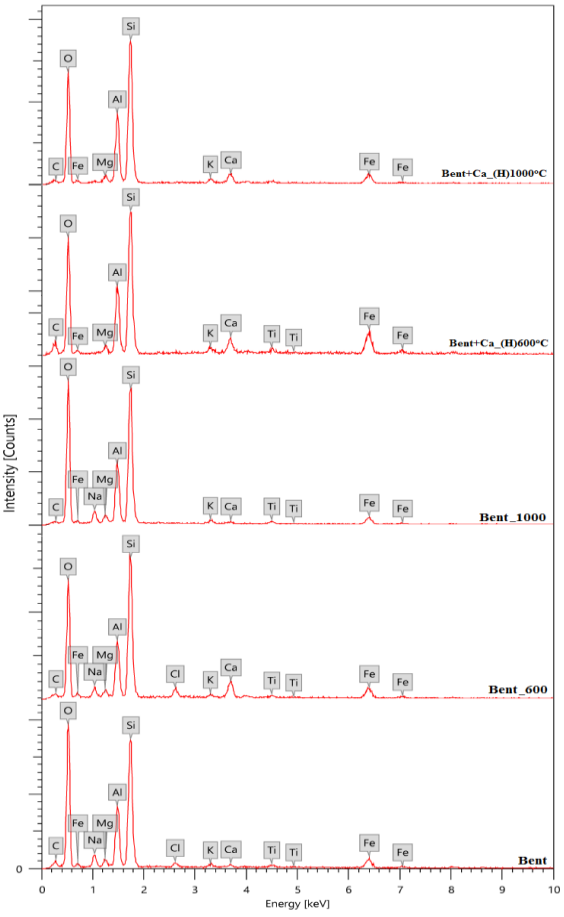

Fig. 7. EDX spectrum of bentonite (Bent) and the hydrothermal (H) treatments ones at 600, and 1000^oC

TABLE 3 The element analysis of bentonite (Bent) and the hydrothermal (H) treatments ones at 600, and 1000^oC by EDX technique of the selected points in Fig. 7

Element	Bent	Bent 600^oC	Bent 1000^oC	Bent+Ca (H) 600^oC	Bent+Ca (H) 1000^oC
C	7.13	3.49	2.13	6.03	2.41
O	50.85	49.70	51.54	49.16	48.49
Na	2.84	2.36	2.87	--	--
Mg	1.18	1.15	1.23	1.17	1.18
Al	9.10	8.73	8.57	9.40	11.23
Si	19.62	21.01	25.76	21.19	25.41
Cl	0.99	1.62	--	--	--
K	0.68	0.67	0.84	0.88	1.48
Ca	1.24	4.53	0.49	2.78	2.65
Ti	0.79	0.73	0.71	1.05	1.36
Fe	5.61	6.05	5.88	8.34	6.48
Si/Al	2.16	2.41	3.01	2.25	2.26

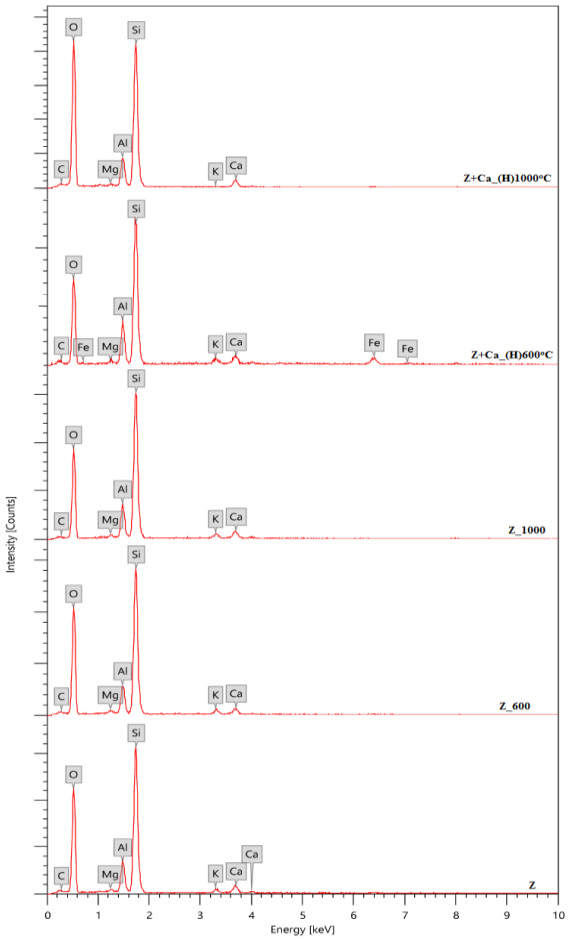

Fig. 8. EDX spectrum of zeolite (Z) and hydrothermal (H) treatments ones at 600 and 1000°C

TABLE . 4 The EDX element analysis of zeolite () and the hydrothermal (H) treatments ones at 600, and 1000°C EDX technique of the selected points in Fig. 8

Element	Z	Z 600°C	Z 1000°C	Z+Ca (H) 600°C	Z+Ca (H) 1000°C
C	5.72	2.91	1.61	2.58	4.44
O	55.00	49.17	46.87	50.24	60.59
Mg	0.48	0.55	0.53	0.78	0.50
Al	5.88	6.78	7.39	8.38	5.59
Si	27.90	34.66	37.71	28.80	26.04
K	1.03	1.83	2.52	1.60	0.56
Ca	2.79	3.17	3.38	3.28	2.31
Fe	1.19	1.07	--	5.34	--
Si/Al	4.74	5.12	5.10	3.44	4.66

In general, As a result of the thermal treatments (200 to 1000°C), the structure of both bentonite and zeolite could be collapsed, destabilized and decreased pore volume, surface area, and interlayer water and that could affect its Premoval ability (Bojemueller et al., 2001; Mulder et al., 2008; Bertagnolli et al., 2011; Nones et al., 2016; Seraj et al., 2016; Torres et al., 2017). Also, studying the charge position and hydration characterizations indicated the importance of layer-charge distribution by thermal treatment on the mobility of interlayer ions and binding preference (Liu et al., 2008). On another side, the results of the hydrothermal treatment indicated the role of the calcium-binding to sorbents on phosphorus removal capacity. Therefore, that could regulate the sorption of phosphorus by associatingwith Ca^{2+}, as well as a stable nuclei source for the formation of Ca-phosphates(Kõiv etal., 2010). However, the removal ability tends to reduce with increasing the heating rate and calcination time due to the pore damage, and the surface area decrease (Mara et al., 2016). Adding $CaCl_2$ beforeHydrothermaltreatments could give more bounded $Ca^{++}$to sorbents than adding $CaCl_2$ after calcination due to pores and surface area reduction.

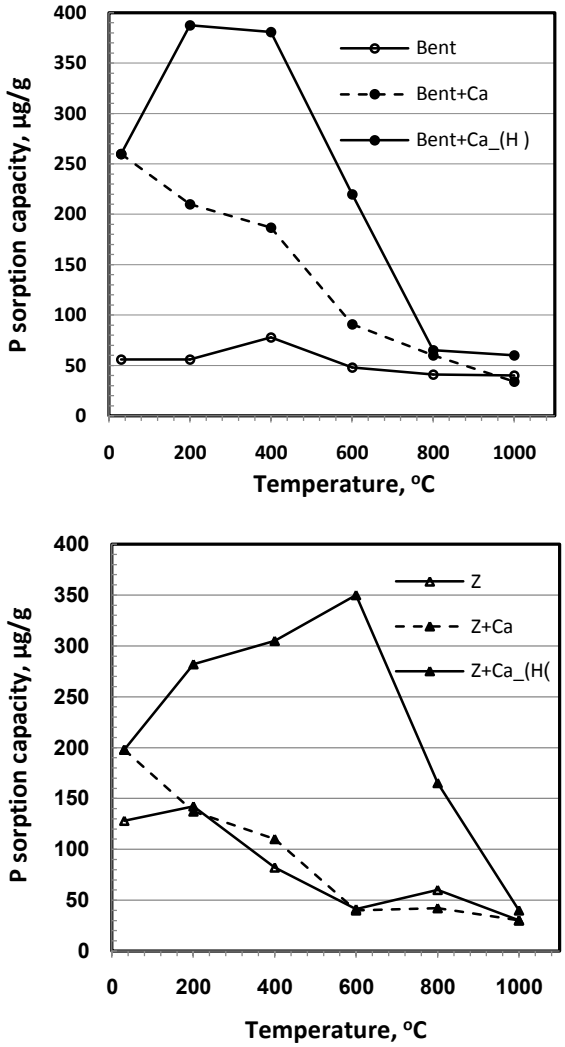

Fig. 9. Effect of thermal treatment for bentonite (Bent) and zeolite (Z) with and without $CaCl_2$ (0.1 M) treatment compared to hydrothermal treatments (H) with $CaCl_2$ (0.1 M) on phosphorus sorption capacity (µg/g)

For bentonite, there was a clear distinction trend between different treatments, and the sorption ability decreased from 387.6, 210, 56 µgP/gfor hydrothermal, calcination with $CaCl_2$, and without $CaCl_2$ at 200^{o}C, respectively, to become (≤50 µgP/g) almost plate from 800 to 1000 ^{o}C. The same trend was observed for calcination zeolite and calcination zeolite treated with $CaCl_2$ to decrease from 137 to 40 µgP/g. otherwise, the removal ability peak of the hydrothermal treatment was 350 µgP/g at 600^{o}C and decreased to 40 µgP/g at 1000^{o}C. Increasing P removal ability at 600^{o}C could be explained by stimulating the structure of zeolite at 600^{o}C in the presence of Ca^{++} ions. Sorption of the phosphate ions by anion exchange could be affected by dealumination occurrence (Gonzalez-Velasco et al., 2000; Elaiopoulos et al., 2010). As indicated by EDX analysis for Zeolite Ca-modification by hydrothermal treatment at 600^{o}C, the surface Si/Al ratio decreased to 3.44 compared to other treatments. The changing of Al^{3+} lattice could change the mineral charge balance (Sposito et al., 1999; Li and Schulthess, 2020); mild structural dealumination could enhance activity sites (Rudham and Winstanley, 1994); beside high Ca^{++} percentage subsequently influences the P removal ability.

Conclusions

The original bentonite and zeolite, and their products of thermal and hydrothermal treatment with $CaCl_2$(0.1M) at different temperatures were characterized by mineralogical, element compositions, and morphological methods. The results showed that increasing temperature affects the structure of bentonite and zeoliteas a result of the dehydration and dehydroxylation process, indicated by the XRD, FTIR, SEM, and EDX analysis. These changes were less in the presence of calcium ions and changing the Si/Al ratioin hydrothermal treatments. All of these changes have affected the P sorption ability of bentonite and zeolite and their thermal treatment products. The sorption abilityof phosphorus decreased with the increasing temperature of the thermal treatment of the sorbents with the privilege for bentonite than zeolite, and Ca-modification by hydrothermal treatment with $CaCl_2$ than calcinated ones and treated after calcination with $CaCl_2$.

Conflicts of interest

"There are no conflicts to declare".

Formatting of funding sources

There is no funding to report for the submission

Acknowledgments

The author thanks Prof. Maher Saleh for his support, helpful cooperation, and offering lab facilities.

References

Ahmaruzzaman M (2008). Adsorption of phenolic compounds on low-cost adsorbents: a review.Adv. *Colloid Interface Sci.,* **143**(1-2), 48–67. https://doi.org/10.1016/j.cis.2008.07.002

Al-Essa K (2018). Activation of Jordanian bentonite by hydrochloric acid and its potential for olive mill wastewater enhanced treatment. *J. Chem.,* 8385692, 1-10. https://doi.org/10.1155/2018/8385692426.8194

Anadão, P, Pajolli, I, Hildebrando, E A, and Wiebeck, H (2014) Preparation and characterization of carbon/montmorillonite composites and nanocomposites from waste bleaching sodium montmorillonite clay. *Adv Powder Technol*, **25**:926–932. https://doi.org/10.1016/j.apt.2014.01.010

Anirudhan T S, Ramachandran M (2015) Adsorptive removal of basic dyes from aqueous solutions by surfactant modified bentonite clay (organoclay): Kinetic and competitive adsorption isotherm. *Process Saf. Environ. Prot..,* **95**, 215–225. http://dx.doi.org/10.1016/j.psep.2015.03.003

Ayari F, Srasra E, Trabelsi-Ayadi M (2007). Removal of lead, zincand nickel using sodium bentonite activated clay. *ASIAN J CHEM.,* **19** (5), 3325–3339.

Benhouria A, Islam A M, Zaghouane-Boudiaf H, Boutahala M, Hameed B H (2015) Calcium alginate–bentonite–activated carbon composite beads as highly effective adsorbent for methylene blue. *Chem. Eng. Sci.,* **270**, 621–630. https://doi.org/10.1016/j.cej.2015.02.030

Bertagnolli C, Kleinübing S J, Silva M G C (2011). Preparation and characterization of a Brazilian bentonite clay for removal of copper in porous beds. Appl. Clay Sci, 53, 73-79. https://doi.org/10.1016/j.clay.2011.05.002

Bloom P R (2000). Soil pH and pH Buffering. p.B333–B352, Handbook of Soil Science, Section B Soil Chemistry (M.E. Sumner, Edtor). CRC Press: Boca Raton, Florida, USA.

Bojemueller E, Nennemann A, Lagaly G (2001). Enhanced pesticide adsorption by thermally modified bentonites. *Appl. Clay Sci.,* **18**, 277–284. https://doi.org/10.1016/S0169-1317(01)00027-8

Byrappa K, Yoshimura M (2013) Handbook of Hydrothermal Technology. William Andrew Inc.https://doi.org/10.1016/C2009-0-20354-0

Chen W J, Hsiao, L C, Chen K Y (2008). Metal desorption from copper (II)/nickel(II)-spiked kaolin as a soil component using plant-derived saponinbiosurfactant. *Process Biochem,* **43** (5), 488-498. https://doi.org/10.1016/j.procbio.2007.11.017

Cinku K, Karakas F, Boylu F (2014). Effect of calcinated magnesite on rheology of bentonite suspensions magnesia-bentonite interaction.

Physicochem. Probl. Miner. Process, **50**(2), 453−466

Claverie M, Martin F, Tardy J P, Cyr M, De Parseval P, Grauby O, Le Roux C(2015). Structural and chemical changes in kaolinite caused by flash calcination: Formation of spherical particles. *Appl. Clay Sci.*, **114**, 247–255. http://dx.doi.org/10.1016/j.clay.2015.05.031

Darweesh H M, Nagieb Z A (2007) Hydration of calcined bentonite Portland blended cement pastes. *Indian J. Chem. Technol*., **14**, 301-307.

D'Eliaa A, Pinto D, Eramo G, Giannossa L C, Ventruti G, Laviano R (2018). Effects of processing on the mineralogy and solubility of carbonate-rich clays for alkaline activation purpose: mechanical, thermal activation in red/ox atmosphere and their combination. *Appl. Clay Sci.*, **152**, 9–21. https://doi.org/10.1016/J.CLAY.2017.11.036

El Refaey A A (2021) Removal of methylene blue dye from aqueous solutions by bentonite and cement kiln dust: comparative study of adsorption equilibrium, kinetic, and thermodynamic. *Alex. Sci. Exch.*, **42**(3), 629- 644. https://doi.org/10.21608/asejaiqjsae.2021.186823

Elaiopoulos K, Perraki T, Grigoropoulou E (2010) Monitoring the effect of hydrothermal treatments on the structure of a natural zeolite through a combined XRD, FTIR, XRF, SEM and N_2-porosimetry analysis. *Microporous Mesoporous Mater.*, **134**, 29–43. https://doi.org/10.1016/j.micromeso.2010.05.004

El-etr W M T, Aly E M, Eid T A (2016) Effect of irrigation regime and natural soil conditioner on crop productivity in sandy soil. *Egyptian Journal of Soil Science*, **56** (2), 327-350. https://doi.org/ 10.21608/EJSS.2016.860

Erdemoğlu M, Birinci M, and Uysal T (2020) Thermal behavior of pyrophyllite ore during calcination for thermal activation for aluminium extraction by acid leaching. *Clays Clay Miner.*, **68** (2), 89–99. https://doi.org/10.1007/s42860-019-00061-w

Gomah H H (2015) In-Situ Remediation of Heavy Metals in Sewage Sludge Using Some Pesticides and Inorganic Amendments. *Egyptian Journal of Soil Science*, **55** (4), 453-462. https://doi.org/ 10.21608/EJSS.2015.1562

Gonzalez-Velasco J R , Lopez-Fonseca R, Aranzabal A, Gutierrez-Ortiz J I, Steltenpohl P (2000). Evaluation of H-type zeolites in the destructive oxidation of chlorinated volatile organic compounds. *Appl. Catal.* B **24**, 233-244. https://doi.org/10.1016/S0926-3373(99)00105-8

Grim R E (1968). Clay Mineralogy, 2nd ed. McGraw-Hill. New York.

Grim R E, Güven N (1978) Bentonites, Geology, Mineralogy, Properties and Uses, Development in Sedimentology.Vol. 24, Elsevier, Amsterdam.

Harvey C C, Lagaly G (2013) Industrial application.p.451–490, Handbook of Clay Science.Elsevier, Amsterdam.

Hilal M H, Helal M M (2013) Role of sulfur in agriculture "phosphate- sulfur bentonite mixture for optimum utilization of rock phosphate as a fertilizer". *Egyptian Journal of Soil Science*, **53** (3), 299-312. https://doi.org/ 10.21608/EJSS.2013.169

IUPAC (1997) Compendium of Chemical Terminology, 2nd ed. (the "Gold Book") Compiled by A. D. McNaught and A. Wilkinson.Blackwell Scientific Publications, Oxford. Online version (2019) created by S. J. Chalk. ISBN 0-9678550-9-8.*https://doi.org/10.1351/goldbook.*

Jowett C, Solntseva I, Wu L, James C, Glasauer S (2018). Removal of sewage phosphorus by adsorptionand mineral precipitation, with recovery as a fertilizingsoil amendment. *Water Sci. Technol.*, **77**, 1976- 1978. https://doi.org/10.2166/wst.2018.027

Kim J R, Kim Y A, Yoon J H, Park D W, Woo H C (2002). Catalytic degradation of polypropylene: effect of dealumination of clinoptilolite catalyst. Polym. *Degrad. Stab*, **75**(2), 287-294.https://doi.org/10.1016/S0141-3910(01)00231-2

Kõiv M, Liira M, ManderÜlo, Mõtlep R, Vohla C, Kirsimäe K (2010). Phosphorus removal using Ca-rich hydrated oil shale ash as filter material-The effect of different phosphorus loadings and wastewater compositions. *Water Res.*, **44**, 5232-5239. https://doi.org/10.1016/j.watres.2010.06.044

Kubilay S, Gürkan R, Savran A, SahanT (2007). Removal of Cu(II), Zn(II) and Co(II) ions from aqueous solutions by adsorption onto natural bentonite. *Adsorption*. **13**, 41–51. https://doi.org/10.1007/s10450-007-9003-y

Kumararaja P, Manjaiaha K M, Datta S C, Sarkar B (2017) Remediation of metal contaminated soil by aluminium pillared bentonite: Synthesis, characterisation, equilibrium study and plant growth experiment. *Appl. Clay Sci.*, **137**, 115–122. https://doi.org/10.1016/j.clay.2016.12.017

Leggo P J, Ledesert B, Christie G (2006) The role of clinoptilolite in organo-zeolitic-soil systems used for phytoremediation. *Sci. Total Environ.*, 363, 1-10. https://doi.org/10.1016/j.scitotenv.2005.09.055

Li Y W, Schulthess C P (2020) Ion-Exchange modeling of monovalent alkali cation adsorption on montmorillonite. *Clays and Clay Minerals*,

68(5), 476–490. https://doi.org/10.1007/s42860-020-00091-9.

Li Z, Jiang W T, Hong H (2008) An FTIR investigation of hexadecyltrimethyl ammonium intercalation into rectorite. *Spectrochim Acta* Part A, **71**, 1525–1534. https://doi.org/10.1016/j.saa.2008.05.015

Liu X, Wang R, Zhou H (2008) Effects of layer-charge distribution on the thermodynamic and microscopic properties of Cs-smectite, *Geochim. Cosmochim. Acta*, **72**, 1837–1847. https://doi.org/10.1016/j.gca.2008.01.028

Lopez-Fonseca R, de Rivas B, Gutierrez-Ortiz J I, Aranzabal A, Gonzalez- Velasco, J R (2003). Enhanced activity of zeolites by chemical dealumination for chlorinated VOC abatement. *Appl. Ca* B, **41** (1-2), 31-42. https://doi.org/10.1016/S0926-3373(02)00199-6

Mara A,Wijaya K, Trisunaryati W, Mudasir (2016). Effect of sulfuric acid concentration of bentonite and calcination time of pillared bentonite. *AIP Conference Proceedings* **1725**, 020042; https://doi.org/10.1063/1.4945496

Moharam S, Jalali M (2015) Use of modified clays for removal of phosphorus from aqueous solutions. *Environ Monit Assess*, **187**: 639. https://doi.org/10.1007/s10661-015-4854-2

Moharam S, Jalali M (2013) Removal of phosphorus from aqueous solution by Iranian natural adsorbents. *Chem. Eng. Sci.*, **223**, 328–339. https://doi.org/10.1016/j.cej.2013.02.114

Mroczkowska-Szerszeń M, Orzechowski M (2018). Infrared spectroscopy methods in reservoir rocks analysis– semi quantitative approach for carbonate rocks. *NAFTA-GAZ*, Nr **11**, 802-812. https://doi.org/10.18668/NG.2018.11.04

Mulder I, Velazquez A L B, Arvide M G T, White G N, Dixon J B (2008) Smectite clay sequestration of aflatoxin b: particle size and morphology. *Clay Clay Miner*, **56**, 558-570. https://doi.org/10.1346/CCMN.2008.0560509

Murat M, Comel C (1983) Hydration reaction and hardening of calcined clays and related minerals III. Influence of calcination process of kaolinite on mechanical strengths of hardened metakaolinite. *Cem Concr Res.*, **13**(5), 631-637.

Murray H (2007 Applied Clay Mineralogy: Occurances, Processing and Application of Kaolins, Bentonites, Palygorskite-sepiolite, and Common Clays. Elsevier, Amsterdam.

Nader M (2015) Surface area: Brunauer–Emmett–Teller (BET). Progress in Filtration and Separation (S. Tarleton, Ed.). p. 585–608, Academic Press, London, UK.

Nakhli S A A, Delkash M, Bakhshayesh B E, Kazemian H (2017) Application of zeolites for sustainable agriculture: a Review on Water and Nutrient Retention. *Water Air Soil Pollut*, **228**, 464.https://doi.org/10.1007/s11270-017-3649-1

Nones J, Nones J, Riella H G, Poli A, Trentin A G, Kuhnen N C (2015). Thermal treatment of bentonite reduces aflatoxin b1 adsorption and affects stem cell death. Mater SciEng C, 55:530–537. https://doi.org/10.1016/j.msec.2015.05.069

Nones J, Nones J, Riella H G, Poli A, Kuhnen N C (2016). Calcination of Brazilian bentonite affects Itsstructural properties and reduces ability to bind Afb1. IJRT. 5(4), 29 – 36.

Novaković T, Rožić L, Petrović S, Rosić A (2008). Synthesis and characterization of acid-activated Serbian smectite clays obtained by statistically designed experiments. *Chem. Eng. Sci.*, **137**, 436–442. https://doi.org/10.1016/j.cej.2007.06.003

O'Hare D (2001) Hydrothermal Synthesis. Encyclopedia of Materials: Science and Technology (2nd ed), p.3989-3992. Elsevier, Amsterdam. https://doi.org/10.1016/B0-08-043152-6/00701-4

Olsen S R, Sommers L E (1982) Phosphorus. In A.L. Page et al. (Ed.) Chemical and microbiological properties.2nd ed. p. 403-427, ASA, Madison, WI.

Paluszkiewicz C, Holtzerb M, Bobrowski A (2008). FTIR analysis of bentonite in moulding sands. *Journal of Molecular Structure*, **880**, 109–114. https://doi.org/10.1016/j.molstruc.2008.01.028

Pavia, D.L., Lampman GM, Kriz GS, Vyvyan, J.R. (2009) Introduction to Spectroscopy, 4th ed. Brooks/Cole, Belmont,CA.

Ravindra R T, Kaneko S, Endo T, Reddy L S (2017). Spectroscopic characterization of bentonite. *J. Laser Opt Photonics*, **4**,171. https://doi.org/10.4172/2469-410X.1000171

Rentz J A, Turner I P, Ullman J L (2009) Removal of phosphorus from solution using biogenic iron oxides, *Water Res.*, **43**(7), 2029–2035. https://doi.org/10.1016/j.watres.2009.02.021

Rossetto E, Beraldin R, Penha F G, Pergher S B C (2009). Characterization of bentonites and diatomite clays and their application as adsorbents. *New Chemistry*, **32**, 2064–2067 (in portuguese). https://doi.org/10.1590/S0100-40422009000800015

Rouquerol J, Avnir D, Faibridge C W, Everett D H, Haynes J H, Pernicone N, Ramsay J D F, Sing K S W, Unger K K (1994). Recommendations for the characterization of porous solids (technical report), *Pure Appl. Chem.*, **66** (8), 1739–1758. https://doi.org/10.1351/pac199466081739

Rudham R, Winstanley A W (1994). Effects of Dry-air Calcination on the Physico-chemical and Catalytic Properties of HZSM-5 Zeolite. *J. CHEM. SOC. FARADAY TRANS.*, **90**(20), 3191-3199.

Salem A, Afshin H, Behsaz H (2012). Removal of lead by using Raschig rings manufactured with mixture of cement kiln dust, zeolite and bentonite, *J. Hazard. Mater.*, 223– 224 13– 23

Santos F R, Bruno H C, Melgar L Z (2019) Use of

bentonite calcined clay as an adsorbent: equilibrium and thermodynamic study of Rhodamine B adsorption in aqueous solution. *Environ. Sci. Pollut. Res.*, **26**, 28622–28632. https://doi.org/10.1007/s11356-019-04641-0

Sellin P, Leupin O (2014) The use of clay as an engineered barrier in radioactive waste management – a review. *Clays and Clay Minerals*, **61**, 477– 498 .

Seraj S, Ferron R D, Juenger M C G (2016) Calcining natural zeolites to improve their effect on cementitious mixture workability. *CemConcr Res.*, **85**, 102–110. http://dx.doi.org/10.1016/j.cemconres.2016.04.002

Shehata N, El-Geundi M S, Ashour E A, Abobeah R (2016) Structural Characteristics of the Egyptian Clay as a Low-Cost Adsorbent. *Inter. J. Chem. Process Engineer. Res.* **3**(2), 35-45. https://doi.org/10.18488/journal.65/2016.3.2/65.2.35.45

Snellings R A, Gualtieri A F, Elsen J (2009). The Rietveld structure refinement of an exceptionally pure sample of clinoptilolite from Ecuador and its Na-, K-, and Ca-exchanged forms. *ZeitschriftfürKristallographie Supplements*: **30**, 395-400. https://doi.org/10.1524/zksu.2009.0058

Sposito G, Skipper N T, Sutton R, Park S H, Soper A K, Greathouse J A (1999) Surface geochemistry of the clay minerals. *Proceedings of the National Academy of Sciences*, **96**, 3358–3364. https://doi.org/10.1073/pnas.96.7.3358

Stagnaro S Y M, Volzone C, Rueda M L (2012) Influence of thermal treatment on bentonite used as adsorbent for Cd, Pb, Zn retention from mono-solute and poly-solute aqueous solutions. Mater. Res,15(4): 549-553

Toor M, Jin B, Dai S, Vimonses V (2015) Activating natural bentonite as a cost-effective adsorbent for removal of Congo-red in wastewater. *J Ind Eng Chem.*, **21**, 653–66. https://doi.org/10.1016/j.jiec.2014.03.033

Torres D, Villarroel-Rocha J, Barrera D, Gutarra A, Sapag K (2017) Effects of the calcination temperature and the load of sodium carboxymethyl cellulose in the synthesis of novel bentonite ceramic foams. *AVANCES Investigación en Ingeniería* **14**, 133-144.https://doi.org/10.18041/1794-4953/avances.1.1292

Udvardi B, Kovács I J, Kónya P, Földvári M, Füri J, Budai F, Falus G, Fancsik T, Szabó, C, Szalai Z, Mihály J (2014) Application of attenuated total reflectance Fourier transform infrared spectroscopyin the mineralogical study of a landslide area, *Hungary. Sediment. Geol.*, **313**, 1–14. https://doi.org/10.1016/j.sedgeo.2014.08.005.

Vieiraa A F, Neto A, Gimenes M L, da Silva M G C (2010). Removal of nickel on Bofe bentonite calcined clay in porous bed. *J. Hazard. Mater.*, **176**, 109–118. https://doi:10.1016/j.jhazmat.2009.10.128

Vohla C, Kõiv M, Bavor H J, Chazarenc F, Mander U (2011) Filter materials forphosphorus removal from wastewater in treatment wetlands—a review, *Ecol. Eng.*, **37**, 70–89. https://doi.org/10.1016/j.ecoleng.2009.08.003

Wei X C, Viadero J R C, Bhojappa V (2008).Phosphorus removal by acid mine drainagesludge from secondary effluents of municipal wastewater treatment plants, *Water Res.*, **42** (13), 3275–3284.https://doi.org/10.1016/j.watres.2008.04.005

Westholm L J (2006) Substrates for phosphorus removal—potential benefits for on-site wastewater treatment? *Water Res*., **40** (1) 23–36.

Wingenfelder U, Nowack B, Furrer G, Schulin R (2005) Adsorption of Pb and Cd by amine-modified zeolite. *Water Res.*, **39**, 3287–3297. https://doi.org/10.1016/j.watres.2005.05.017

Xiong W H, Peng J (2008) Development and characterization of ferrihydrite-modified diatomite as a phosphorus adsorbent. *Water Res.*, **42**(19), 4869 - 4877. https://doi.org/10.1016/j.watres.2008.09.030

Yahya A M, Al-Qodah, Z, Ngah CW Z (2015) Agricultural bio-waste materials as potential sustainable precursors used for activated carbon production: A review. Renew. *Sust.Energ. Rev.*, **46**, 218–235. https://doi.org/10.1016/j.rser.2015.02.051

Yin H, Yun Y, Zhang Y, Fan C (2011).Phosphate removal from wastewaters by a naturally occurring, calcium-rich sepiolite. *J. Hazard. Mater.*, **198**, 362–369. https://doi.org/10.1016/j.jhazmat.2011.10.072

Yoshimura M, Byrappa K (2008) Hydrothermal processing of materials: past, present and future. *J. Mater. Sci.*, **43** , 2085-2103. https://doi.org/10.1007/s10853-007-1853-x

Zhang J, Wang Z, Li T, Wang Z, Zhang S, Zhong M, Liu Y, Gong X (2019) Preparation of CaO-containing carbon pellet from recycling of carbide slag: Effects of temperature and H_3PO_4. *Waste Manage*, **84**, 64–73. https://doi.org/10.1016/j.wasman.2018.11.033